



Mechanical criteria and sensitivity analysis of water inrush through a mining fault above confined aquifers

Jian Sun^{1,2} · Lianguo Wang² · Yang Hu²

Received: 20 December 2017 / Accepted: 17 December 2018 / Published online: 28 December 2018
© Saudi Society for Geosciences 2018

Abstract

A mechanical model of water inrush through a mining fault in the workface above confined aquifers was developed according to ground pressure and strata control theory. Based on limit equilibrium theory of rock mass, mechanical criteria of the water inrush through the mining fault in the workface above confined aquifers were deduced by considering Mohr–Coulomb yield criterion. Five influencing factors, namely fault dip, fault cohesion, fault internal friction angle, suspended goaf range behind the workface, and thickness of floor strata protective zone, were selected from the mechanical criteria of an ultimate hydraulic pressure that the stope floor strata with a fault can tolerate. An orthogonal test was performed to analyze the sensitivity of the ultimate hydraulic pressure tolerated by the stope floor strata with fault. Results show that the fault dip and thickness of the floor strata protective zone significantly influence the ultimate hydraulic pressure tolerated by the stope floor strata with fault and represent 32.8% and 32.5% of the total effects, respectively. The fault cohesion, fault internal friction angle, and suspended goaf range behind the workface exert similar effects on the ultimate hydraulic pressure that the floor strata with a fault can tolerate and comprise 10.5%, 13.5%, and 10.7% of the total effects, respectively. The ultimate hydraulic pressure that the stope floor strata with a fault can tolerate decreases with the increase in the fault dip, fault internal friction angle, and suspended goaf range behind the workface but increases with the fault cohesion and thickness of the floor strata protective zone. This property decreases with the distance between the coal wall of the workface and the fault. This study provides insights into the water inrush mechanism through the mining fault in the workface and its corresponding sensitivity, thereby aiding in establishing the safe mining of coal seam with fault above confined aquifers.

Keywords Water inrush through fault · Ultimate hydraulic pressure · Mechanical criteria · Sensitivity

Introduction

The geological conditions in China are extremely complex that geological disasters occasionally occur in coal mines despite abundant coal reserves in this country (Gao et al. 2018; Guo et al. 2017; Miao et al. 2004; Qian et al. 2003a). The mining workface encounters increasing threats from Ordovician karst water from coal seam floor with the increase in depth and intensity of coal mines. The prediction and prevention of water inrush in the mining workface with fault structure are novel

research topics (Lu and Wang 2015; Sun et al. 2017; Sun and Miao 2017; Wu and Zhou 2008; Yin et al. 2016; Zhang 2005; Zhang et al. 2014, 2017; Zhou et al. 2017; Zhu and Wei 2011). Water inrush in mines causes not only considerable economic loss and casualties but also severe pollution and damage to local water resources and the environment (Bai and Miao 2009; Du et al. 2017; Miao 2011). Therefore, effective prevention of mine water disasters and technological problems that numerous mines face has become a research issue.

A fault-activated water inrush is a major form of mine water inrush. This type of phenomenon exhibits a robust concealment and indefinability and can easily cause severe disasters, thereby significantly threatening the safety of coal mining. Statistics reveal that 80% of mine water inrush accidents in China are caused by fault activation. Most of these accidents are caused by mining-induced activation of nonconductive fault under original geological conditions (Han et al. 2009; Hu et al. 2014; Liang et al. 2015; Li et al. 2011, 2017; Liu et al. 2017; Shi and Singh 2001; Wu et al. 2004).

✉ Jian Sun
sj323@cumt.edu.cn

¹ School of Energy and Safety, Anhui University of Science and Technology, Huainan 232001, Anhui, China

² State Key Laboratory of Coal Resources and Safe Mining, China University of Mining and Technology, Xuzhou 221116, Jiangsu, China

Li et al. (1996) studied the water inrush mechanism theoretically through stope floor fault by using a structural key strata model of water inrush from the seam floor and proposed evaluation criteria to understand the mechanism of fault-activated water inrush. On the basis of “practical ground pressure control” theory, Song et al. (2013) theoretically examined the causes of the rapid increase in floor karstic water and problems in traditional mine water control by considering a mining-induced strata movement and effects of ground pressure on karst water pressure and fault pillar. These authors developed a predictive control mechanical model and relevant control criteria of cross-fault mining. Lu et al. (2014) deduced the analytical expression of the hydraulic pressure of water inrush from the seam floor under the influence of fault by considering the combined effect of mining and hydraulic pressures of a confined aquifer beneath the floor. In addition, these authors identified the most risky shear failure plane and critical water inrush pressure on the floor through a trial method and analyzed the effects of the distance between the open-off cut of the workface and the fault zone, fault dip, advancing direction of the workface, and lateral pressure coefficients on the critical water inrush pressure on the floor.

Based on water-resisting key strata, Li et al. (2009) established an activated mechanical model of water-resisting key strata with waterproof fault and analyzed the fault activation slippage conditions of a waterproof fault under the influence of the mining and hydraulic pressures. Huang et al. (2010) discussed the effects of a fault on the stability of water-resisting floor and deduced the formula of a critical hydraulic pressure for waterproof failure. These authors also analyzed the effects of the fault dip, fault cohesion, and width of fault coal pillar on the failure of the water-resisting floor. These studies play a critical role in understanding the fault-activated water inrush mechanism and predicting fault water inrush.

In a coal mining design, protective coal pillars are generally set in faults with large falls to avoid the influence of mining. The faults in the fully mechanized coal mining workface generally possess small falls. Water inrush, which is caused by activating buried structures (e.g., small fault), has a robust concealment and high control difficulties. Numerous researchers have investigated the setting of water-resisting coal pillars in faults with large falls. However, systematic studies on water inrush mechanism caused by small-fault mining in the workface, its influencing factors, and evolution laws remain lacking. The literature also lacks a quantitative sensitivity analysis of the influencing factors of mining-induced fault water inrush.

Thus, the mechanical model of water inrush through the mining fault in the workface above confined aquifers was developed on the basis of ground pressure and strata control theory. The mechanical criteria of water inrush through the mining fault in the workface above confined aquifers were deduced. An orthogonal test was performed to analyze the effects and sensitivity of the fault dip, fault cohesion, fault internal friction

angle, suspended goaf range behind the workface, thickness of floor strata protective zone, and distance from the coal wall of the workface to the fault on the ultimate hydraulic pressure that the stope floor strata with fault can tolerate. The present study provides insights into the water inrush mechanism through the mining fault in the workface and its corresponding sensitivity, which can aid in establishing the safe mining of coal seam with fault above confined aquifers.

Mechanical model of water inrush through the mining fault in the workface

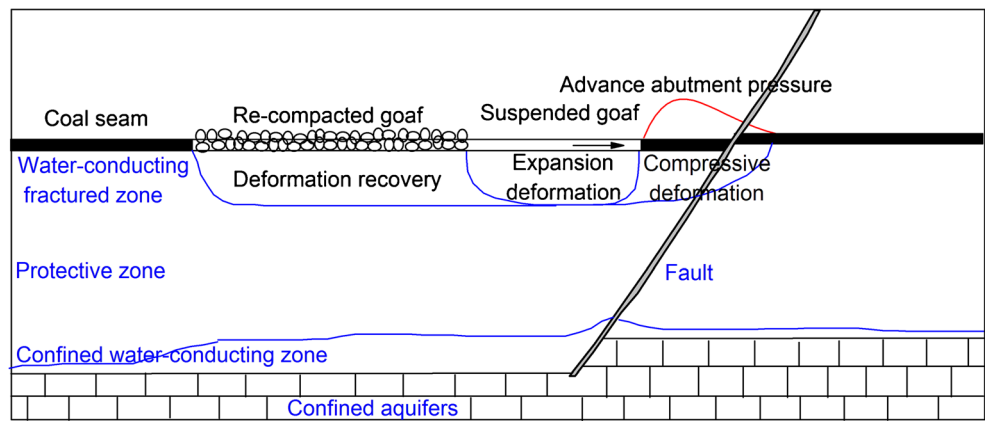
Engineering background

Water-conducting fractures have been developed upward at different heights on the top interface of floor-confined aquifers before mining coal seam with fault above confined aquifers. This setup is known as the original confined water-conducting zone, whose height is generally small. The floor strata in front of the workface produce compressive deformation under the action of the advance abutment pressure of the workface during mining of the workface. The compressed and deformed floor strata produce expansion deformation given the release of pressure when the workface pushes through this region. Numerous damage cracks can be generated in this region after releasing pressure and expanding the floor strata, thereby forming a water-conducting fractured zone with a certain depth in the floor strata, which has water-conducting capacity, as depicted in Fig. 1. Thus, the water-conducting fractured zone is formed by the compressive deformation zone after releasing pressure from the floor strata. Owing to the advancement of the workface, the overlying strata of a goaf will fall behind the workface, and the fallen gangue will re-compact the expanded and deformed goaf floor strata. Moreover, the expansion and deformation of the goaf floor strata will be recovered.

Therefore, the workface floor strata during mining of coal seam with fault above confined aquifers undergo the following three stages: pre-mining stress concentration, post-mining pressure relief and expansion, and stress recovery. The three stages correspond to pre-mining compressive deformation, post-mining expansion deformation, and deformation recovery of floor strata, as illustrated in Fig. 1. The fault in the workface can easily be activated during mining, thereby leading to developing the fault fracture zone. The confined water under the collaborative effect of mining and hydraulic pressures of confined water may further rise along the original confined water-conducting and fault fracture zones, thus forming a confined water-conducting zone with different heights. Therefore, a wavy interface was used to demonstrate the height of the confined water-conducting zone in Fig. 1.

The overlying strata of the goaf behind the workface are in a state of suspension, and the goaf floor strata are in a state of

Fig. 1 Deformation failure of floor strata and confined water-conducting rise during mining of coal seam with fault above confined aquifers



pressure relief and expansion before the expanded and deformed goaf floor strata are re-compacted by the fallen gangue. Fault water inrush may occur in the workface when the confined water-conducting and fault fracture zones connect with the water-conducting fractured zone. Therefore, the goaf floor with fault beneath the suspended goaf behind the workface is a dangerous region with easy water inrush before the fault occurs on the mining workface.

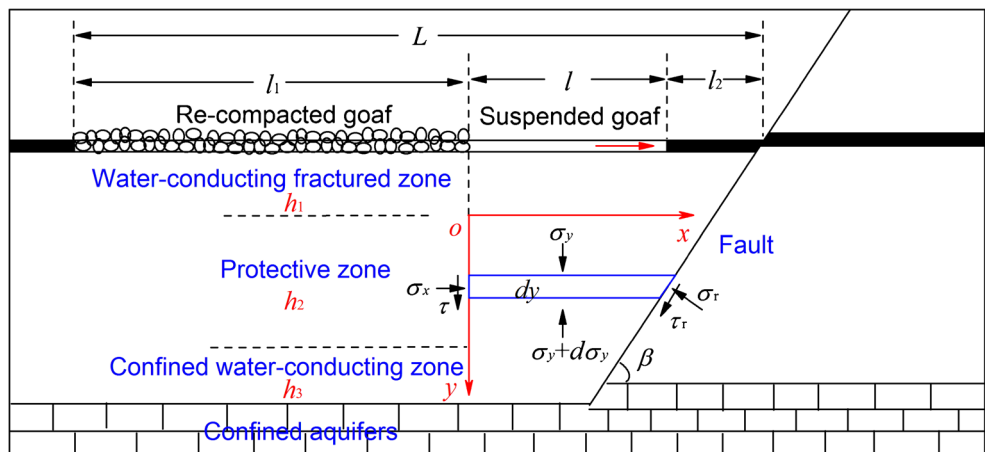
Mechanical criteria

Water inrush from the coal seam floor is a common problem in underground coal seam mining, and the mechanism of water inrush is complex. Water inrush from the floor may be caused by the expansion of cracks in the mining floor and the communication of confined aquifers. Water inrush from the floor may also be caused by activating geological structures, such as faults and fall columns, and penetrating mining space. In terms of the position of water inrush from the floor, water inrush can occur from the floor in front of the workface, from the floor in the workface, and from the goaf floor behind the workface. Owing to the complexity of the mechanism of water inrush from the floor, analyzing all of the problems of water inrush from the floor with a single model is infeasible, but

examining only the mechanism of water inrush from the floor for certain geological conditions and mining environments is feasible.

Mining fault activation forms the fault fracture zone, destroys the floor strata integrity, and reduces the waterproof performance of the floor strata protective zone. The stability and water-isolating capacity of the floor strata with a fault under simultaneous effect of mining and hydraulic pressures of confined water is assessed. According to ground pressure and strata control theory (Qian et al. 2003b), a mechanical model of water inrush through the mining fault in the workface above confined aquifers was constructed, as depicted in Fig. 2. The “inverted trapezoidal” differential units with a thickness dy were selected in the protective zone of the stope floor with a fault along the advancing direction of the workface presented in Fig. 1. The mechanical model focuses on investigating the ultimate hydraulic pressure that the stope floor strata with fault can tolerate and its influencing factors and sensitivity when a fault occurs in the mining workface. In Fig. 2, L is the distance from the open-off cut in the workface to the fault, l is the range of suspended goaf behind the workface, l_1 is the range of re-compacted goaf by caved overburden behind the workface, and l_2 is the distance from the coal wall of the workface to the fault.

Fig. 2 Mechanical model of water inrush through the mining fault in the workface above confined aquifers



This study mainly investigates the problem of water inrush prediction for the stope floor with fault during mining of the workface. The goaf floor with fault beneath the suspended goaf behind the workface is the dangerous region with easy water inrush before the fault occurs on the mining workface. Therefore, a rectangular coordinate system was established, as displayed in Fig. 2. In this figure, a coordinate axis in the rectangular coordinate system is set at the boundary position of the suspended goaf behind the workface. Simultaneously, the x -axis is set at the interface position between the water-conducting fractured and protective zones of the floor strata and orients to the same direction of the workface movement to analyze the influence of the thickness of the floor protective zone on the water inrush through the mining fault in the workface. Otherwise, given the shape of the “inverted trapezoidal” differential units, the y -axis is set at the interface position between the suspended goaf behind the workface and the re-compacted goaf by the caved overburden and orients downward and perpendicular to the floor strata. This process aims to analyze the influence of the suspended goaf range behind the workface and the distance from the coal wall of the workface to the fault on the water inrush through the mining fault in the workface. The origin o is the intersection of the x - and y -axes.

The water pressure in the confined water-conducting zone beneath the suspended goaf floor is not much different before water inrush from the mining floor with the fault, although the height of the confined water-conducting zone of the stope floor with fault is different. Therefore, in the force analysis of the mechanical model of water inrush through the mining fault in the workface above confined aquifers, the water pressure in the confined water-conducting zone beneath the suspended goaf floor is simplified to a uniform water pressure. The floor strata with fault beneath the suspended goaf possess balanced stresses before water inrush through the mining fault in the workface. According to ultimate balance theory of rock mass (Li et al. 1991), the force analysis of “inverted trapezoidal” differential units with a thickness dy is determined, as exhibited in Fig. 2.

In Fig. 2, the horizontal stress σ_x and shearing strength τ of the protective zone strata influence the left-end face of the differential units. The vertical stress σ_y and increment $\sigma_y + d\sigma_y$ affect the upper and lower surfaces. The shearing strength τ_r and the normal stress σ_r of fault surface influence the right-

end bevel. The “inverted trapezoidal” differential units with a thickness dy along the x and y directions satisfy

$$\left. \begin{aligned} \sigma_x dy &= \sigma_r \sin\beta \frac{dy}{\sin\beta} + \tau_r \cos\beta \frac{dy}{\sin\beta} \\ \sigma_y l + \pi dy + \tau_r \sin\beta \frac{dy}{\sin\beta} &= (\sigma_y + d\sigma_y) \left(l - \frac{dy}{\tan\beta} \right) + \sigma_r \cos\beta \frac{dy}{\sin\beta} \end{aligned} \right\} \quad (1)$$

correspondingly, where β is the fault dip.

According to ultimate balance theory of rock mass, the “inverted trapezoidal” differential units will shear slide upward along the fault surface in the process of fault activation and water inrush. The left-end face of the differential units during this process will be affected by the horizontal stress σ_x and shearing strength τ of the protective zone strata, and the right-end bevel will be affected by the normal stress σ_r and shearing strength τ_r of the fault surface, as presented in Fig. 2. According to Mohr–Coulomb yield criterion, the shearing strength τ of the protective zone strata and shearing strength τ_r of the fault surface satisfy

$$\left. \begin{aligned} \tau &= C + \sigma_x \tan\varphi \\ \tau_r &= C_r + \sigma_r \tan\varphi_r \end{aligned} \right\} \quad (2)$$

where C and φ are the cohesion and internal friction angle of the protective zone strata, respectively; C_r and φ_r are the cohesion and internal friction angle of the fault surface, correspondingly.

In Fig. 2, the horizontal stress σ_x and vertical stress σ_y on the fault surrounding rock are assumed to be the minimum and maximum principal stresses, respectively. Accordingly, the normal stress σ_r on the fault surface can be expressed as follows:

$$\sigma_r = \frac{\sigma_x + \sigma_y}{2} + \frac{\sigma_x - \sigma_y}{2} \cos 2\beta \quad (3)$$

According to the Mohr–Coulomb yield criterion, the ultimate equilibrium conditions of rock mass failure are

$$\frac{\sigma_y + C \cot\varphi}{\sigma_x + C \cot\varphi} = \frac{1 + \sin\varphi}{1 - \sin\varphi} \quad (4)$$

The following expression can be obtained by substituting Eqs. (2)–(4) into Eq. (1):

$$\left. \begin{aligned} l d\sigma_y + \left[\frac{(1 - \sin\varphi)(\cot\beta - \tan\varphi_r)}{(1 + \sin\varphi)(1 + \cot\beta \tan\varphi_r)} - \frac{(1 - \sin\varphi)\tan\varphi}{1 + \sin\varphi} - \frac{1}{\tan\beta} \right] \sigma_y dy - \frac{dy}{\tan\beta} d\sigma_y \\ - \left\{ \frac{[2C \cos\varphi + C_r(1 + \sin\varphi)\cot\beta](\cot\beta - \tan\varphi_r)}{(1 + \sin\varphi)(1 + \cot\beta \tan\varphi_r)} - \frac{2C \sin\varphi}{1 + \sin\varphi} + C + C_r \right\} dy = 0 \end{aligned} \right\} \quad (5)$$

The second-order differential component $dyd\sigma_y$ is omitted, and the two sides of Eq. (5) are divided by dy . Thus, Eq. (5) can be further simplified to

$$\frac{d\sigma_y}{dy} + \left[\frac{(1-\sin\varphi)(\cot\beta-\tan\varphi_r)}{(1+\sin\varphi)(1+\cot\beta\tan\varphi_r)} - \frac{(1-\sin\varphi)\tan\varphi}{1+\sin\varphi} - \frac{1}{\tan\beta} \right] \frac{\sigma_y}{l} - \left\{ \frac{[2C\cos\varphi + C_r(1+\sin\varphi)\cot\beta](\cot\beta-\tan\varphi_r)}{(1+\sin\varphi)(1+\cot\beta\tan\varphi_r)} - \frac{2C\sin\varphi}{1+\sin\varphi} + C + C_r \right\} \frac{1}{l} = 0 \tag{6}$$

The following expression can be obtained by integrating Eq. (6):

$$\sigma_y = Ae^{-\frac{B_1}{l}y} + \frac{B_2}{B_1} \tag{7}$$

where A is the integration constant to be determined, and

$$B_1 = \frac{(1-\sin\varphi)(\cot\beta-\tan\varphi_r)}{(1+\sin\varphi)(1+\cot\beta\tan\varphi_r)} - \frac{(1-\sin\varphi)\tan\varphi}{1+\sin\varphi} - \frac{1}{\tan\beta}$$

$$B_2 = \frac{[2C\cos\varphi + C_r(1+\sin\varphi)\cot\beta](\cot\beta-\tan\varphi_r)}{(1+\sin\varphi)(1+\cot\beta\tan\varphi_r)} - \frac{2C\sin\varphi}{1+\sin\varphi} + C + C_r$$

In Eq. (7), $\sigma_y = \gamma_1 h_1$ when $y = 0$, where h_1 is the depth of the water-conducting fractured zone, and γ_1 is its bulk density. Thus, the integration constant $A = \gamma_1 h_1 - B_2/B_1$. $\sigma_y = P_c - (\gamma_1 h_1 + \gamma_2 h_2)$ when $y = h_2$, where P_c is the hydraulic pressure of progressively confined water-conducting rise, h_2 is the thickness of the floor protective zone, and γ_2 is the bulk density. P_c can be obtained as follows by substituting these values into Eq. (7):

$$P_c = \left(\gamma_1 h_1 - \frac{B_2}{B_1} \right) e^{-\frac{B_1}{l}h_2} + \frac{B_2}{B_1} + (\gamma_1 h_1 + \gamma_2 h_2) \tag{8}$$

Certain hydraulic pressure loss occurs during the upward progressive conducting rise of confined water. Such hydraulic pressure loss is closely related to the permeability of floor strata. Poor permeability will cause considerable hydraulic pressure losses. Hydraulic pressure loss is negatively related to the permeability coefficient of floor strata. Research has reported that $\eta = 0.0906\exp(-14.969k)$, where η is the hydraulic pressure loss, and k is the permeability of floor strata (Yin and Hu 2008). $P_c = P_0 - h_3\eta$, where P_0 is the hydraulic pressure of floor-confined aquifer, and h_3 is the height of the confined water-conducting zone of the floor. Therefore, the mechanical criterion for water inrush through the mining fault in the workface above confined aquifers is

$$P_0 \geq P_m \tag{9}$$

where P_m is the ultimate hydraulic pressure that the stope floor strata with a fault can tolerate, and

$$P_m = \left(\gamma_1 h_1 - \frac{B_2}{B_1} \right) e^{-\frac{B_1}{l}h_2} + \frac{B_2}{B_1} + (\gamma_1 h_1 + \gamma_2 h_2) + h_3\eta \tag{10}$$

Thus, the mining fault in the workface under the collaborative effect of the mining and hydraulic pressures of the confined water becomes unstable when $P_0 > P_m$, thereby inducing water inrush through the fault. The mining fault in the workface reaches the critically unstable state when $P_0 = P_m$, and water inrush can be induced through the fault. The mining fault in the workface is stable when $P_0 < P_m$, and water inrush cannot be induced through the fault.

Sensitivity analysis of water inrush through the mining fault in the workface

Multi-factor analysis

A fully mechanized workface for coal seam mining is generally 80–200 m long. The stope roof is managed by a full caving method. The range of suspended goaf behind the fully mechanized workface is 20–50 m. The depth of the floor water-conducting fractured zone that was formed after workface mining ranges from 5 to 25 m. Geological data from floor drilling in coal seam revealed that the height of the floor-confined water-conducting zone is 0–15 m.

The probability for the mining fault in the workface to develop shear failure along the fault surface decreases with the reduction in the fault dip because of the influence of the structural surface dip on the rock mass strength. The fault failure is mainly caused by transverse expansion of the fault surface when the fault dip is large, especially approaching 90° (Li et al. 1991). Therefore, the present study focused on fault-activated water inrush when the fault dip and its influencing factors range between 30 and 75°.

In addition, the internal friction angle of rock in coal measure stratum is mainly concentrated in the range of 20–50° (Qian et al. 2003b). For complete sandstone, limestone, sandy

shale, and other hard rock, the internal friction angle is mostly in the range of 30–50°. Moreover, for certain broken soft rocks, such as mudstone, shale, and sandy mudstone, the internal friction angle is mostly within the range of 20–35°. The effect of the internal friction angle of the fault on the water inrush from the activated fault is analyzed, and the fault zone is relatively broken after activating the fault. At present, the study range of the internal friction angle of the fault was extended from 10 to 40°. Simultaneously, the internal friction angle of the floor protective zone was determined to range from 20 to 50°. The detailed parameter ranges of a fully mechanized workface for coal seam mining with the fault above confined aquifers are listed in Table 1.

Based on the formula of the ultimate hydraulic pressure P_m that the stope floor strata with fault can tolerate, five main influencing factors, namely fault dip β , fault cohesion C_r , fault internal friction angle φ_r , suspended goaf range behind the workface l , and thickness of the floor protective zone h_2 , were selected from Table 1. The parameter range of the five main influencing factors (i.e., β , C_r , φ_r , l , and h_2) was equally divided into four levels using the $L_{16}(4^5)$ orthogonal test program to analyze the effects of these influencing factors on the ultimate hydraulic pressure P_m that the stope floor strata with a fault can tolerate. Tables 2 and 3 summarize the calculation results of the ultimate hydraulic pressure P_m with the orthogonal test program and the other calculation parameters for P_m , correspondingly.

Table 2 demonstrates that only the ultimate hydraulic pressure P_m in the orthogonal test Schemes 3, 4, 5, 11, and 12 are higher than 3.5 MPa when the hydraulic pressure of the stope floor-confined aquifer is 3.5 MPa, thereby indicating that these design schemes are reliable and will not induce water inrush through mining faults.

Table 1 Parameter ranges of mining workface with fault above confined aquifers

Parameters	Symbol	General range
Dip angle of fault in workface	β	30~75/°
Range of suspended goaf behind workface	l	20~50/m
Distance from coal wall of workface to fault	l_2	0~60/m
Depth of water-conducting fractured zone	h_1	5~25/m
Thickness of floor protective zone	h_2	5~20/m
Height of confined water-conducting zone	h_3	0~15/m
Water pressure of floor-confined aquifer	P_0	0~5/MPa
Bulk density of water-conducting fractured zone	γ_1	5~35/kN.m ⁻³
Bulk density of floor protective zone	γ_2	5~35/kN.m ⁻³
Cohesive strength of floor protective zone	C	1~5/MPa
Internal friction angle of floor protective zone	φ	20~50/°
Cohesive strength of fault	C_r	0~0.4/MPa
Internal friction angle of fault	φ_r	10~40/°
Hydraulic pressure loss	η	0~0.1/MPa.m ⁻¹

Table 2 Ultimate hydraulic pressure P_m that the stope floor strata with a fault can tolerate calculated by the $L_{16}(4^5)$ orthogonal test program

No.	Parameter values of $L_{16}(4^5)$ orthogonal design					Water pressure P_m /MPa
	β /°	C_r /MPa	φ_r /°	l /m	h_2 /m	
1	30	0.1	10	20	5	2.898
2	30	0.2	20	30	10	3.378
3	30	0.3	30	40	15	3.586
4	30	0.4	40	50	20	3.672
5	45	0.1	20	40	20	3.503
6	45	0.2	10	50	15	2.907
7	45	0.3	40	20	10	2.836
8	45	0.4	30	30	5	1.993
9	60	0.1	30	50	10	1.958
10	60	0.2	40	40	5	1.689
11	60	0.3	10	30	20	3.773
12	60	0.4	20	20	15	3.635
13	75	0.1	40	30	15	1.816
14	75	0.2	30	20	20	2.596
15	75	0.3	20	50	5	1.686
16	75	0.4	10	40	10	2.110

The summed values $\sum P_{mi}$ ($i = 1, 2, 3,$ and 4) and their corresponding average values $\overline{\sum P_{mi}}$ ($i = 1, 2, 3,$ and 4) of P_m under four levels of the five influencing factors (β , C_r , φ_r , l , h_2) were calculated. The calculations were performed to analyze the effects of five main influencing factors on the ultimate hydraulic pressure P_m that the stope floor strata with a fault can tolerate. The results are presented in Table 4, where R is the range, and $R = \max \overline{\sum P_{mi}} - \min \overline{\sum P_{mi}}$ ($i = 1, 2, 3,$ and 4). R represents the variation amplitude of the experimental results when a factor changes. R in Table 4 indicates that β mostly affects P_m , followed by h_2 , φ_r , l , and C_r successively. Among these factors, β and h_2 represent 65.3% of the total impacts, that is, 32.8% and 32.5%, respectively. φ_r , l , and C_r exert similar effects on P_m , thus comprising 13.5%, 10.7%, and 10.5% of the total effects, respectively.

Variations in the effects of the five influencing factors (β , C_r , φ_r , l , and h_2) with average values $\overline{\sum P_{mi}}$ ($i = 1, 2, 3,$ and 4) are depicted in Fig. 3. Figure 3 intuitively reflects the change law of the ultimate hydraulic pressure P_m that the stope floor strata with a fault can tolerate when the five main influencing factors (i.e., β , C_r , φ_r , l , and h_2) change. That is, the ultimate hydraulic pressure P_m and speed of the ultimate hydraulic pressure P_m can be increased or decreased when the five main

Table 3 Other calculation parameters for P_m

h_1 /m	h_3 /m	γ_1 /kN.m ⁻³	γ_2 /kN.m ⁻³	C /MPa	φ /°	η /MPa.m ⁻¹
15	10	25	28	2	30	0.07

Table 4 Analysis of results calculated by the $L_{16}(4^5)$ orthogonal test program

Orthogonal parameters	ΣL_1	ΣL_2	ΣL_3	ΣL_4	$\overline{\Sigma L_1}$	$\overline{\Sigma L_2}$	$\overline{\Sigma L_3}$	$\overline{\Sigma L_4}$	R	Effect degree (%)
β	13.534	11.239	11.055	8.208	3.384	2.810	2.764	2.052	1.332	32.8
C_r	10.175	10.570	11.881	11.410	2.544	2.643	2.970	2.853	0.426	10.5
φ_r	11.688	12.202	10.133	10.013	2.922	3.050	2.533	2.503	0.547	13.5
l	11.965	10.960	10.888	10.223	2.991	2.740	2.722	2.556	0.435	10.7
h_2	8.266	10.282	11.944	13.544	2.067	2.571	2.986	3.386	1.319	32.5

influencing factors change. An increased or decreased speed of ultimate hydraulic pressure P_m indicates a significant effect of the influencing factor.

Figure 3 illustrates that the average value $\overline{\Sigma P_{mi}}$ decreases rapidly with the increase in the fault dip β , thereby indicating that the ultimate hydraulic pressure P_m tolerated by the stope floor strata with a fault is negatively related to the fault dip. Average value $\overline{\Sigma P_{mi}}$ generally increases, except for a small reduction in the late period, when the fault cohesion C_r increases. This result is mainly caused by the small thickness of the floor protective zone h_2 in orthogonal test Scheme 8. Average value $\overline{\Sigma P_{mi}}$ decreases slightly in the late period because h_2 significantly influences the orthogonal test results. If h_2 increases, then P_m will increase while C_r increases. This result is analyzed in “Single-factor analysis.” Average value $\overline{\Sigma P_{mi}}$ generally declines with the increase in the fault internal friction angle φ_r , thereby reflecting a negative relationship between P_m and φ_r . However, the minimal increase in P_m in the early stage is mainly attributed to the thick floor protective zone h_2 in the orthogonal test Scheme 5. If h_2 decreases, then P_m will decrease while φ_r increases.

Average value $\overline{\Sigma P_{mi}}$ declines gradually with the increase in the suspended goaf range behind the workforce l . The ultimate

hydraulic pressure P_m that the stope floor strata with a fault can tolerate is therefore negatively correlated with l . A large suspended goaf range behind the workforce causes high risks of water inrush through mining fault. Average value $\overline{\Sigma P_{mi}}$ increases linearly with the increase in the thickness of the floor protective zone h_2 , thus indicating that P_m is positively correlated to h_2 . A thick floor protective zone is conducive to obstructing water inrush through mining fault.

Single-factor analysis

1. Fault dip

Owing to the parameter values in Table 5, the relationship of the ultimate hydraulic pressure P_m that the stope floor strata with a fault can tolerate and the fault dip β is exhibited in Fig. 4. The ultimate hydraulic pressure P_m nonlinearly decreases when the fault dip β increases, thereby indicating that a large fault dip causes a low ultimate hydraulic pressure tolerated by the stope floor strata with fault. Thus, a large dip fault can easily cause water inrush through mining fault caused by fault activation.

Fig. 3 Variations of the effects of the five influencing factors with the average value of each level

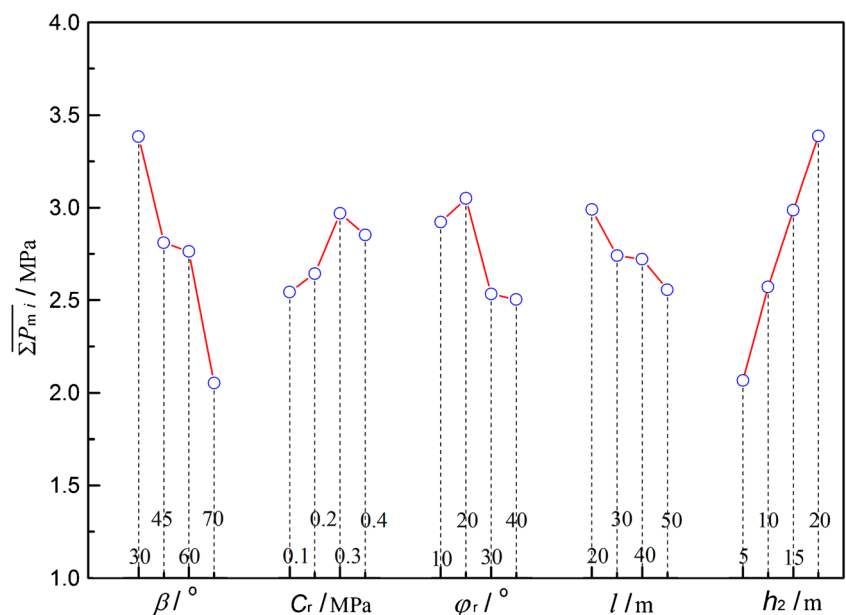


Table 5 Physical and mechanical properties of the stope floor rock strata with fault

$h_1/$ m	$h_2/$ m	$h_3/$ m	$l/$ m	$\gamma_1/$ kN.m^{-3}	$\gamma_2/$ kN.m^{-3}	$\eta/$ MPa.m^{-1}	$C/$ MPa	$\varphi/$ $^\circ$	$C_r/$ MPa	$\varphi_r/$ $^\circ$	$\beta/$ $^\circ$
15	20	10	40	25	28	0.07	2	30	0.3	20	45

2. Mechanical properties of fault

Figure 5 illustrates the variations in the effects of the ultimate hydraulic pressure P_m that the stope floor strata with a fault can tolerate on the fault cohesion C_r and fault internal friction angle φ_r when other parameter values presented in Table 5 are considered. The ultimate hydraulic pressure P_m nearly increases linearly with the increase in fault cohesion C_r , as depicted in Fig. 5a. Based on Mohr–Coulomb yield criterion, with the increase of fault cohesion C_r , the strength of fault would increase. And the stability of the floor strata with fault improves with the increase in the fault cohesion, which can aid in preventing the water inrush through the mining fault.

By contrast, the ultimate hydraulic pressure P_m that the stope floor strata with a fault can tolerate decreases with the increase in fault internal friction angle φ_r , as displayed in Fig. 5b. Studies have shown that a large internal friction angle of rock denotes a fragile rock, which is vulnerable to brittle damage. On the one hand, the rock with small internal friction angle is soft, and further plastic deformation occurs (Sun et al. 2013). Thus, the hard rock layer can resist strong deformation but easily form water-conducting fracture after breaking. On the other hand, the soft rock layer has a high deformation tendency but is minimally susceptible to destruction because the soft rock can seal the fractures generated in the

hard rock, thus increasing its capability to prevent water flow. Therefore, the ultimate hydraulic pressure that the stope floor strata with a fault can tolerate deteriorates when the internal friction angle of fault increases, thereby simplifying the occurrence of water inrush through the mining fault.

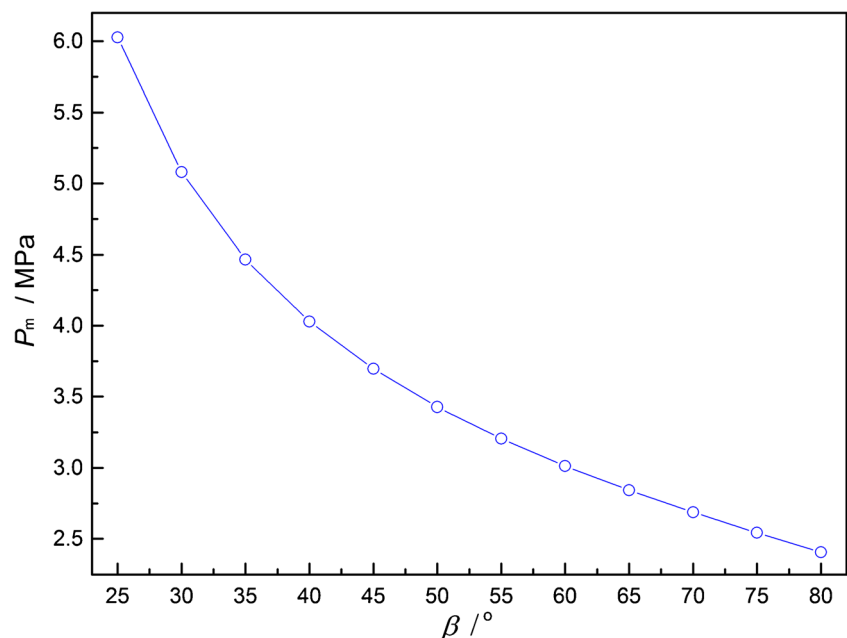
3. Range of suspended goaf behind the workface

Figure 6 depicts the variations in the effects of the ultimate hydraulic pressure P_m that the stope floor strata with a fault can tolerate on the suspended goaf range l behind the workface when the other parameter values displayed in Table 5 are fixed. The ultimate hydraulic pressure P_m decreases nonlinearly with the increase in l . Therefore, a large suspended goaf range will reduce the ultimate hydraulic pressure tolerated by the floor rock strata with fault and is disadvantageous for the stability control of the floor strata with fault. This condition can easily induce water inrush through the mining fault in the stope.

4. Thickness of the floor protective zone

Figure 7 presents the variations in the effects of the ultimate hydraulic pressure P_m that the stope floor strata with a fault can tolerate on the thickness of the floor protective zone h_2 when the other parameter values displayed in Table 5 are

Fig. 4 Relationship of the ultimate hydraulic pressure P_m that the stope floor strata with a fault can tolerate and the fault dip β



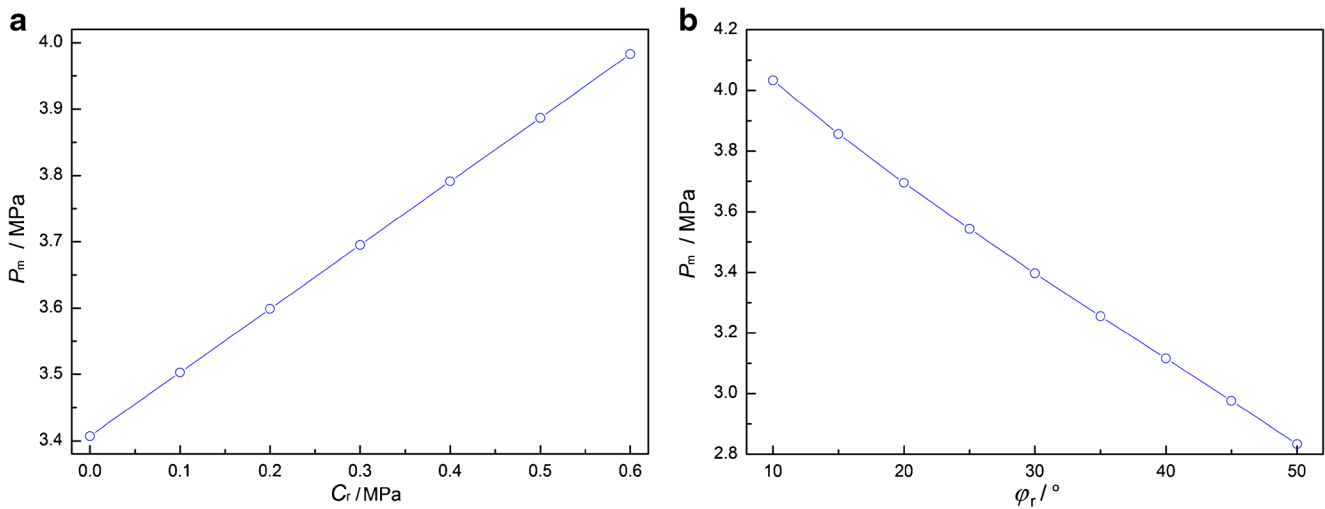


Fig. 5 Variations in the effects of the ultimate hydraulic pressure P_m that the stope floor strata with a fault can tolerate on (a) fault cohesion C_r and (b) fault internal friction angle φ_r

fixed. The ultimate hydraulic pressure P_m nearly increases linearly with the increase in h_2 . This result reveals that a thick floor protective zone is accompanied by a high ultimate hydraulic pressure that the stope floor strata with a fault can tolerate. This condition is conducive to obstructing water inrush through the mining fault.

5. Distance from the coal wall of the workface to the fault

According to field monitoring, fault activation can be observed when the coal wall of the workface is approximately 60 m away from the fault. The fault activation and failure range increase accordingly with the continuous improvement of the workface. The range of the suspended goaf behind the

workface is expressed as $l = L - l_1 - l_2$, as depicted in Fig. 2, to determine the effects of the distance l_2 between the coal wall of the workface and the fault on the ultimate hydraulic pressure P_m that the stope floor strata with a fault can tolerate.

Figure 8 demonstrates the variations in the effects of the ultimate hydraulic pressure P_m that the stope floor strata with a fault can tolerate on the distance l_2 from the coal wall of the workface to the fault when the other parameter values listed in Table 5, that is, $L = 150$ m and $l_1 = 50$ m, are fixed. The ultimate hydraulic pressure P_m decreases nonlinearly with the reduction in l_2 . Therefore, a short distance from the coal wall of the workface to the fault can reduce the ultimate hydraulic pressure that the stope floor strata with a fault can tolerate, thus easily inducing water inrush through the mining fault.

Fig. 6 Variations in the effects of the ultimate hydraulic pressure P_m that the stope floor strata with a fault can tolerate on the suspended goaf range l behind the workface

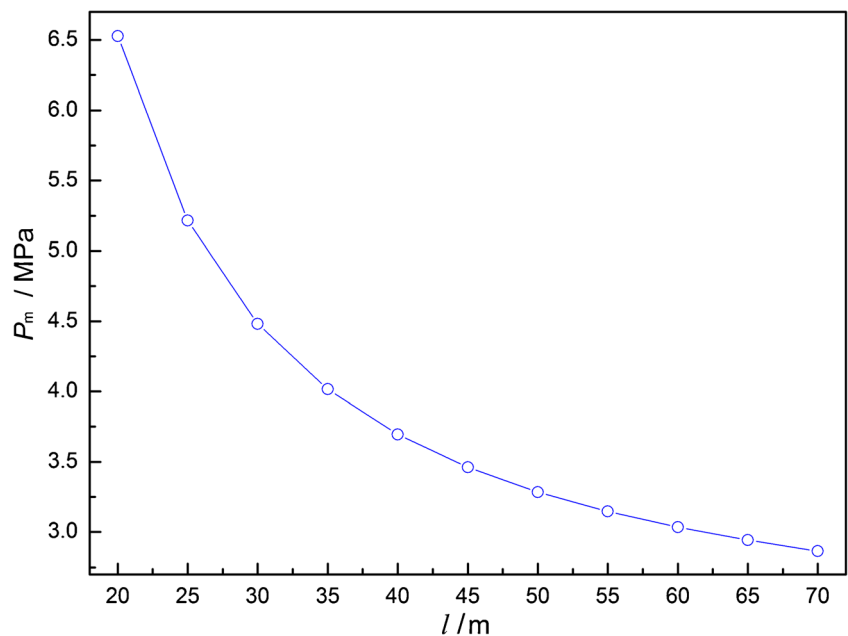
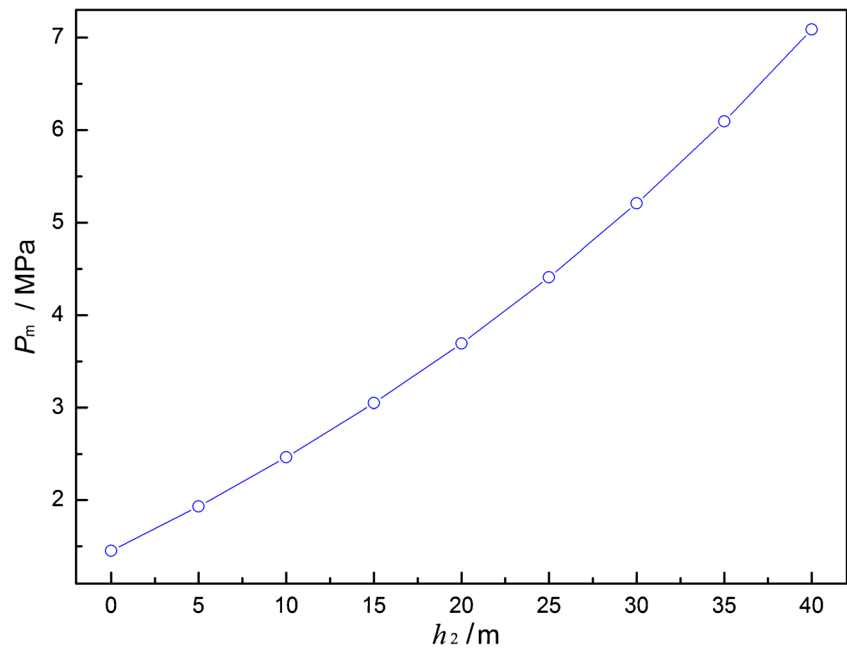


Fig. 7 Variations in the effects of the ultimate hydraulic pressure P_m that the stope floor strata with a fault can tolerate on the thickness of the floor protective zone h_2



Therefore, most mines establish fault protective coal pillars with a certain width to prevent the water inrush through faults.

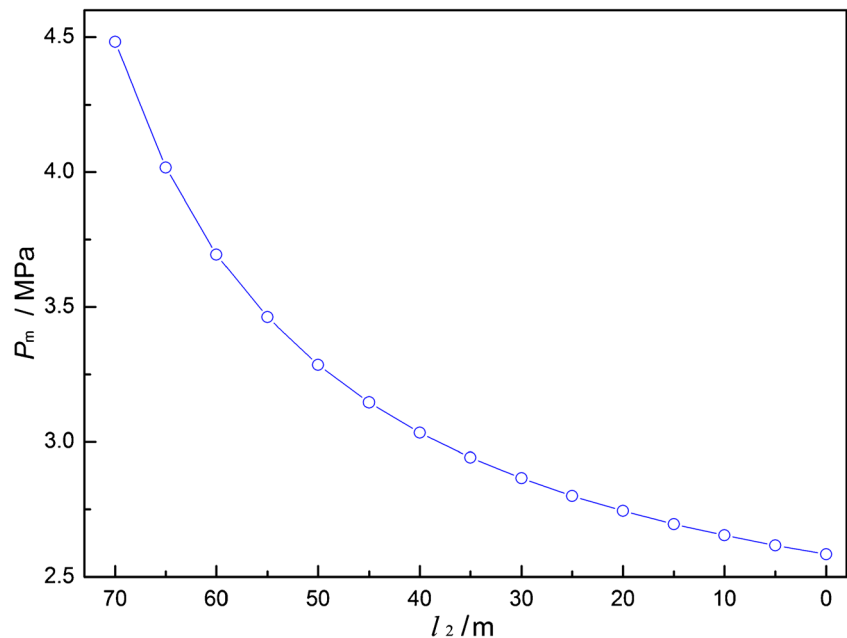
6. Fault throw

Water inrush caused by fault activation in the coal measure stratum demonstrates a robust concealment and uncertainty. In particular, a small fault in the mining workface exhibits strong invisibility and considerable difficulty in preventing and controlling the activation of water inrush, thereby seriously threatening the safety of the production of a coal mine. Water inrush caused by fault activation in the mining workface is the result

of simultaneous mining stress and water pressure in confined aquifers. The influencing factors include mining stress, aquifer water pressure, fault dip, fault cohesion, fault internal friction angle, suspended goaf range behind workface, and thickness of floor strata protective zone; in addition, fault throw, fault type, mining depth, advance direction of the workface, and other factors influence the characteristic parameters of fault surrounding rock and activation of water inrush in the fault.

The mechanical model of water inrush through the mining fault in the workface above confined aquifers (Fig. 2) established in this study does not reflect the effect of fault

Fig. 8 Variations in the effects of the ultimate hydraulic pressure P_m that the stope floor strata with a fault can tolerate on the distance l_2 between the coal wall of the workface and the fault



throw on the activation of water inrush in the fault. However, Fig. 2 demonstrates that fault throw can change the distance between the mining coal seam workface and the opposite confined aquifers. The increased fault throw shortens the distance between the mining workface and the opposite confined aquifers and reduces the thickness of the effective water-resisting strata of the floor. The confined water in the opposite confined aquifers may flow directly along the fault fractured zone into the mining workface, thereby resulting in water inrush from the stope floor with fault.

Conclusions

A mechanical model of water inrush through a mining fault in the workface above confined aquifers was developed in accordance with ground pressure and strata control theory. On the basis of limit equilibrium theory of rock mass, the mechanical criteria of water inrush through the mining fault in the workface above confined aquifers were deduced by considering the Mohr–Coulomb yield criterion.

Five influencing factors, namely fault dip, fault cohesion, fault internal friction angle, suspended goaf range behind the workface, and thickness of the floor strata protective zone, were selected from the mechanical criteria of the ultimate hydraulic pressure that the stope floor strata with a fault can tolerate. An orthogonal test was conducted to analyze the sensitivity of the ultimate hydraulic pressure tolerated by the stope floor strata with fault. The results show that the fault dip and thickness of the floor strata protective zone significantly influence the ultimate hydraulic pressure tolerated by the stope floor strata with fault and represent 32.8% and 32.5% of the total effects, respectively. The fault cohesion, fault internal friction angle, and suspended goaf range behind the workface exert similar effects on the ultimate hydraulic pressure that the floor strata with a fault can tolerate and comprise 10.5%, 13.5%, and 10.7% of the total effects, correspondingly.

The ultimate hydraulic pressure that the stope floor strata with a fault can tolerate decreases nonlinearly with the increase in the fault dip and range of suspended goaf behind the workface but nearly increases linearly with the fault cohesion and thickness of the floor protective zone. Then, the ultimate hydraulic pressure tolerated by the stope floor strata with the fault nearly decreases linearly when the internal friction angle of the fault increases, and when the distance from the coal wall of the workface to the fault decreases.

Acknowledgments This study was supported by the National Natural Science Foundation of China (No. 51404013, No. 51674008), the Open Projects of State Key Laboratory of Coal Resources and Safe Mining at China University of Mining and Technology (No. 19KF01), the Major Research Funding Project of Natural Science of Anhui Province

University (No. KJ2018ZD010), and the Natural Science Foundation of Anhui Province (No. 1508085ME77, No. 1708085ME133).

References

- Bai HB, Miao XX (2009) Research progress and major problems of water preserved coal mining. *J Min Saf Eng* 26(3):253–262
- Du WS, Jiang YD, Ma ZQ, Jiao ZH (2017) Assessment of water inrush and factor sensitivity analysis in an amalgamated coal mine in China. *Arab J Geosci* 10(21):471
- Gao R, Yan H, Ju F, Mei XC, Wang XL (2018) Influential factors and control of water inrush in a coal seam as the main aquifer. *Int J Min Sci Technol* 28(2):187–193
- Guo BH, Cheng T, Wang L, Luo T, Yang XY (2018) Physical simulation of water inrush through the mine floor from a confined aquifer. *Mine Water Environ* 37(3):577–585.
- Han J, Shi LQ, Yu XG, Wei JC, Li SC (2009) Mechanism of mine water-inrush through a fault from the floor. *Min Sci Technol* 19(3):276–281
- Hu XY, Wang LG, Lu YL, Yu M (2014) Analysis of insidious fault activation and water inrush from the mining floor. *Int J Min Sci Technol* 24(4):477–483
- Huang CH, Feng T, Wang WJ, Liu H (2010) Research on the failure mechanism of water-resisting floor affected by fault. *J Min Saf Eng* 27(2):219–222
- Li TL, Tan XS, Liu CW (1991) *Rock mechanics for mine*. Chongqing University Press, Chongqing
- Li LJ, Qian MG, Li SG (1996) Mechanism of water-inrush through faults. *J China Coal Soc* 21(2):119–123
- Li QF, Wang WJ, Zhu CQ, Peng WQ (2009) Analysis of fault water inrush mechanism based on the principle of water-resistant key strata. *J Min Saf Eng* 26(1):87–90
- Li LC, Yang TH, Liang ZZ, Zhu WC, Tang CA (2011) Numerical investigation of groundwater outbursts near faults in underground coal mines. *Int J Coal Geol* 85(3–4):276–288
- Li H, Bai HB, Wu JJ, Wang CS, Ma ZG, Du YB (2017) Mechanism of water inrush driven by grouting and control measures—a case study of Chensilou mine, China. *Arab J Geosci* 10(21):468
- Liang DX, Jiang ZQ, Guan YZ (2015) Field research: measuring water pressure resistance in a fault-induced fracture zone. *Mine Water Environ* 34(3):320–328
- Liu SL, Liu WT, Yin DW (2017) Numerical simulation of the lagging water inrush process from insidious fault in coal seam floor. *Geotech Geol Eng* 35(3):1013–1021
- Lu YL, Wang LG (2015) Numerical simulation of mining-induced fracture evolution and water flow in coal seam floor above a confined aquifer. *Comput Geotech* 67: 157–171
- Lu HF, Shen D, Yao DX, Hu YB (2014) Analytical solution of critical water inrush pressure of mining floor affected by fault. *J Min Saf Eng* 31(4):888–895
- Miao XX (2011) *Water preserved coal mining method and application to arid and semi-arid mining areas*. China University of Mining and Technology Press, Xuzhou
- Miao XX, Liu WQ, Chen ZQ (2004) *Seepage theory of mining rockmass*. Science Press of China, Beijing
- Qian MG, Miao XX, Xu JL, Mao XB (2003a) *Key strata theory in ground control*. China University of Mining and Technology Press, Xuzhou
- Qian MG, Shi PW, Xu JL (2003b) *Ground pressure and strata control*. China University of Mining and Technology Press, Xuzhou
- Shi LQ, Singh RN (2001) Study of mine water inrush from floor strata through faults. *Mine Water Environ* 20(3):140–147
- Song ZQ, Hao J, Tang JQ, Shi YK (2013) Study on water inrush from fault's prevention and control theory. *J China Coal Soc* 38(9):1511–1515

- Sun J, Miao XX (2017) Water-isolating capacity of an inclined coal seam floor based on the theory of water-resistant key strata. *Mine Water Environ* 36(2):310–322
- Sun J, Wang LG, Hou HQ (2013) Resurch on water-isolating capacity of the compound water-resisting key strata in coal seam floor. *J China Univ Min Technol* 42(4):560–566
- Sun J, Hu Y, Zhao GM (2017) Relationship between water inrush from coal seam floors and main roof weighting. *Int J Min Sci Technol* 27(5):873–881
- Wu Q, Zhou WF (2008) Prediction of groundwater inrush into coal mines from aquifers underlying the coal seams in China: vulnerability index method and its construction. *Environ Geol* 55(4):245–254
- Wu Q, Wang MY, Wu X (2004) Investigations of groundwater bursting into coal mine seam floors from fault zones. *Int J Rock Mech Min Sci* 41(4):557–571
- Yin SX, Hu WY (2008) Rocks' water-resistance ability and natural progressive intrusion height. *Coal Geol Explor* 36(1):34–36
- Yin HY, Wei JC, Lefticariu L, Guo JB, Xie DL, Li ZL, Zhao P (2016) Numerical simulation of water flow from the coal seam floor in a deep longwall mine in China. *Mine Water Environ* 35(2):243–252
- Zhang JC (2005) Investigations of water inrushes from aquifers under coal seams. *Int J Rock Mech Min Sci* 42(3):350–360
- Zhang R, Jiang ZQ, Zhou HY, Yang CW, Xiao SJ (2014) Groundwater outbursts from faults above a confined aquifer in the coal mining. *Nat Hazards* 71(3):1861–1872
- Zhang SC, Guo WJ, Li YY, Sun WB, Yin DW (2017) Experimental simulation of fault water inrush channel evolution in a coal mine floor. *Mine Water Environ* 36(3):443–451
- Zhou QL, Herrera J, Hidalgo A (2017) The numerical analysis of fault-induced mine water inrush using the extended finite element method and fracture mechanics. *Mine Water Environ* 36(4):1–11
- Zhu WC, Wei CH (2011) Numerical simulation on mining-induced water inrushes related to geologic structures using a damage-based hydro-mechanical model. *Environ Earth Sci* 62(1):43–54